Application of an electronic nose coupled with fuzzy-wavelet network for the detection of meat spoilage

Kodogiannis, V.

This is an author's accepted manuscript of an article published in Food and Bioprocess Technology, doi: 10.1007/s11947-016-1851-6 in 2017.

The final publication is available at Springer via:

https://dx.doi.org/10.1007/s11947-016-1851-6

Application of an electronic nose coupled with fuzzy-wavelet network for the detection of meat spoilage

Vassilis S. Kodogiannis

Faculty of Science and Technology, University of Westminster

115 New Cavendish Street, London W1W 6UW, United Kingdom

V.Kodogiannis@westminster.ac.uk

Abstract:

Food product safety is one of the most promising areas for the application of electronic noses. During the last twenty years, these sensor-based systems have made odour analyses possible. Their application into the area of food is mainly focused on quality control, freshness evaluation, shelf-life analysis and authenticity assessment. In this paper, the performance of a portable electronic nose has been evaluated in monitoring the spoilage of beef fillets stored either aerobically or under modified atmosphere packaging, at different storage temperatures. A novel multi-output fuzzy wavelet neural network model has been developed, which incorporates a clustering pre-processing stage for the definition of fuzzy rules. The dual purpose of the proposed modelling approach is not only to classify beef samples in the relevant quality class (*i.e*. fresh, semi-fresh and spoiled), but also to predict their associated microbiological population. Comparison results against advanced machine learning schemes indicated that the proposed modelling scheme could be considered as a valuable detection methodology in food microbiology.

Keywords:

Fuzzy wavelet neural networks, system identification, principal components analysis, meat spoilage, neural networks, clustering, classification

1. Introduction

One of the most commonly consumed food item worldwide is meat. However, meat's shelf life is low and the consumption of spoiled meat products can easily cause serious health hazards. The development of reliable systems to determine safety/quality of meat products would certainly benefit the public enormously, and also prevent unnecessary economic losses. Although beef is considered as a good source for essential nutrients, it is also a perfect "environment" for the growth of pathogenic microorganisms and consequently spoilage.

Currently, meat safety is mainly relied on regulatory inspection and sampling protocols. This methodology, however, seems insufficient as 100% inspection and sampling is simple difficult to be achieved. Additionally, although a plethora of chemical and microbiological methods have been proposed for the detection and measurement of bacterial meat spoilage, the majority of them are considered as time-consuming processes (Ellis, *et al.,* 2001). Thus, the development and application of rapid and non-invasive sensors for spoilage detection is very desirable for Meat Industry. Various methods based on analytical instrumental techniques, such as Fourier transform infrared spectroscopy (FTIR) (Amamcharla, *et al.,* 2010), Raman spectroscopy (Meisel, *et al.,* 2014) and Hyperspectral Imaging (Tao, *et al.,* 2014) have been investigated for their potential in assessing meat quality.

In the past two decades, consideration of food safety from the point of specific bacteria has resulted in the need for an alternative detection system for microbial spoilage by inspecting volatile organic compounds (VOCs) generated by these microorganisms (Boothe, *et al.,* 2002). The application of human nose as a smell assessment instrument is rather restricted by the fact that our sense of smell is subjective and is therefore difficult to use. Consequently, there was need for an instrument that could "mimic" the human sense of smell and its use in routine industrial applications. To support such technology for industrial usage, gas/odour sensors became ideal candidates in areas like food industry, environment control, automobile industry, indoor air quality check and monitoring and medicine (Capelli, *et al.,* 2014), (Fend, *et al.,* 2006).

The electronic nose (enose) is a system initially created to "mimic" the function of human nose. An enose consists of an array of chemical gas sensors with broad and partly overlapping selectivity that measure volatile compounds (VCs), a signal-preparation system, and a pattern-recognition system. Such device is usually characterised by reproducibility and reliability, as it has a short reaction and recovery time. Although the instrument does not allow the actual identification of compounds and has a higher detection limit against GC–MS, it has been successfully used in processing monitoring, shelf-life investigation, freshness evaluation and authenticity assessment in a wide range of food products (Di Natale, *et al.,* 1998).

The main applications of enose with respect to meat are in assessing quality, spoilage identification and detection of off-flavours. In one of the earliest related studies, the changes in the headspace of vacuum packaged beef, vaccinated with *Salmonella typhimurium*, was evaluated using a metal oxide (MOS) based enose (Balasubramanian, *et al.,* 2008). The VCs of pork and meat products such as sausages were also studied for Halal verification (Nurjuliana, *et al.,* 2011). An enose, consisting of 18 MOS gas sensors, has been used for measuring flavour quality changes of refined chicken fat during controlled oxidation and partial least squares regression (PLS) was utilised as a prediction model (Song, *et al.,* 2013). An olfactory system has been considered for the detection of Salmonella contamination in packaged beef steaks using neural network classifiers (Khot, *et al.*, 2012). The prediction of total viable counts (TVC) in chilled pork using an enose and support vector machine (SVM) has been also investigated. In this specific experiment, enose and microbiological measurements were carried out on pork samples stored at 4 °C for up to 10 days (Wang, *et al.,* 2012).

Adulteration detection of meat has attracted growing attention in recent years. In this perspective, enose was utilised to detect pork adulteration in minced mutton (Tian, *et al.,* 2013).

The main objective of this paper is to associate, for the first time according to literature, volatile fingerprints of odour profile with beef spoilage through a multi-input-multi-output (MIMO) clustering-based fuzzy wavelet neural network (CFWNN) system. The proposed CFWNN system classifies beef fillets stored either aerobically or under modified atmosphere packaging to one of three quality classes (*i.e.* fresh, semi-fresh, and spoiled) and simultaneously predicts the microbial load (as total viable counts – TVC) on meat surface, based on the biochemical profile provided by the enose dataset. Results from CFWNN scheme are compared against models based on Adaptive Neural Fuzzy Inference System (ANFIS), Multilayer Neural Networks (MLP), Support Vector Machines (SVM) as well as linear (PLS) regression schemes. Such comparison is considered as a essential test, as we have to emphasise the need of induction to the area of food microbiology, advanced learning-based modelling schemes, which may have a significant potential for the accurate estimation of meat spoilage.

2. Experimental case

2.1 Sample Preparation and Microbiological Analysis

The entire experimental case study was performed at the Agricultural University of Athens, Greece. A detailed description of the experimental methodology, as well as the related microbiological analysis of the meat samples, is described in (Papadopoulou, *et al.,* 2013). Briefly, the samples were prepared by cutting fresh beef fillers into small pieces and then stored aerobically (AIR) and in modified atmosphere packaging (MAP) (40% CO_2, 30% O_2, 30% N_2) at different temperatures. More specifically, these samples were stored under controlled isothermal conditions at 0, 4, 8, 12, 16 and 20°C in high precision incubators for up to 434 h, depending on storage temperature, until spoilage was observed (Christiansen, *et al*., 2011). After appropriate time intervals during storage, duplicate samples were collected for microbiological, sensory and enose analysis. It was assumed that the microbial population at these parts would be comparable and samples were not subjected to any prior pre-processing such as fat and connective tissue removal. Meat samples stored at aerobic conditions were analyzed every 24, 24, 12 and 8 h for 0, 4, 8 and 12°C respectively. Finally, samples stored at 16 and 20°C were analyzed at 4–6 h intervals. Similarly, samples stored at MAP conditions were analyzed every 48, 24, 16, 12, 8 and 6 h for 0, 4, 8, 12, 16 and 20°C respectively. In parallel, microbiological analysis was performed and resulting growth data were $\log_{10}$ transformed and fitted to the primary model of Baranyi in order to verify the kinetic parameters of microbial growth (maximum specific growth rate and lag phase duration) (Papadopoulou, *et al.,* 2013).

Figure 1

The growth curves of TVC for beef fillet storage at different temperatures under aerobic and MAP conditions as a function of storage time are illustrated in Fig. 1. A close inspection, however, reveals that the maximum specific growth rate (μmax) for the AIR packaged condition is different than of that of the MAP case. It has been found that packaging under modified atmosphere delay the growth rates of all members of the microbial association, as well as the maximum population attained by each microbial group compared with aerobic storage. Aerobic storage increases the rate of spoilage due to the fast growing *Pseudomonas* spp.; in addition such growth can be considerably inhibited by the presence of gas carbon dioxide (Skandamis, *et al*., 2002). Analysis specified that the total viable counts ranged from $3.058 - 9.885 \log_{10}$ cfu cm^{-2} for aerobic cases, and $3.146 - 8.063 \log_{10}$ cfu cm^{-2} for MAP cases. However, for both aerobic and MAP packaging conditions, the growth rate is increased faster, as the storage temperature increases.

Additionally, sensory evaluation of samples was performed during storage, based on the observation of colour and smell before and after cooking (Papadopoulou, *et al.,* 2013). Each sensory attribute was assigned to a three-point scale corresponding to: 1=fresh (acceptable meat quality and the absence of off-flavors); 2=semi-fresh (presence of slight off-flavors but not spoiled); and 3= spoiled (clearly off-flavor development). In total, 210 meat samples were evaluated by a sensory panel and classified into the selected three groups as fresh (n = 48), semi-fresh (n = 72), and spoiled (n = 90) for the aerobic case, while 213 meat samples were classified as fresh (n = 51), semi-fresh (n = 84), and spoiled (n = 78) for the MAP case.

2.2 Volatile Samples Acquisition

Libra enose (Fig. 2) is a portable device produced by Technobiochip and is used to identify complex odours (Di Natale, *et al.,* 2001). The instrument is composed by an array of chemical sensors and a data analysis system. The integrated data analysis system "transforms" the extracted information from an odour to an "olfactory" image, similarly with our sense of a smell. The detection of odours is then based on the concept that different odours have different "olfactory" images. This distinguishes enose from gas chromatography which identifies single molecular classes inside a gaseous mixture. Enose recognises an odour as a whole, showing the synergic activity of different molecular species in a single "olfactory" image.

Figure 2

This sensing device uses a set of eight 20MHz piezoelectric transducers placed in a measuring chamber. The measuring chamber is held at a constant temperature during the measurements by a thermostatic electronic system, while a flow system formed by a micro-electric valve and a micro-pump transmits the gas sample to the measuring chamber. For each measurement, a beef fillet sample of 5 g was introduced inside a 100 ml volume glass jar and left at room temperature (20°C ±2°C) for 15 min to enhance desorption of volatile compounds from the meat into the headspace. The headspace was then pumped over the sensors of the enose and the generated signal was recorded to a computer.
Datasets related to volatile extracted information from Libra enose as well as the associated microbiological analysis from meat samples for both aerobic and MAP cases, were provided by Agricultural University of Athens, Greece and were further utilised towards the development of the proposed intelligent model.

3. CFWNN Architecture

In the current study, a novel Multi-Input Multi-Output (MIMO) Clustering-based Fuzzy Wavelet Neural Network system (CFWNN) has been developed to predict the microbial load (as TVC) on meat surface, based on the biochemical profile provided by the enose dataset. In addition, the same model can classify beef samples to one of three quality classes (*i.e.* fresh, semi-fresh, and spoiled).

Wavelets are known to have good modelling properties over a range of frequencies; hence they have been utilised in neuro-fuzzy (NF) systems (Kodogiannis, *et al.,* 2013). Generally, the fuzzy wavelet neural network (FWNN) is a combined structure based on fuzzy rules that includes wavelet functions in their consequent parts, in the form of a wavelet neural network. In these FWNN schemes, such combination is achieved through a Takagi–Sugeno–Kang (TSK) architecture, which allows us to model nonlinear behaviour with relatively fast training speed. The domain interval of each input is split into fuzzy regions and each region is associated with a membership function (MF) in the IF part of the fuzzy rules. The rules are then learnt adaptively similarly to ANFIS scheme (Abiyev, *et al.,* 2008). The number of fuzzy rules at FWNN scheme is an important issue, as it affects the accuracy and the efficiency of the

developed prediction system. A second problem however is related with the initialization stage. In fact, network's initial parameters definition affects the accuracy result, the time required for learning and even the convergence of the training process.

Figure 3

The proposed CFWNN model differs from traditional FWNN approaches that utilise the "look-up table" concept. In those models, an input space is divided into $K_1 \times K_2 \times .... \times K_n$ fuzzy subspaces, where K_i, $i = 1,2,..,n$, is the number of fuzzy subsets for the i^{th} input variable (Nelles, 2000). The Adaptive Neuro-Fuzzy Inference System (ANFIS) is an example of such approach, where the number of fuzzy rules is associated to the number of input variables as well as the number of MF for each input. In the case of CFWNN, a clustering algorithm is applied for the sample data in order to organize feature vectors into clusters. The fuzzy rule base is then derived using results obtained from a clustering algorithm. In the proposed scheme, the number of memberships for each input variable is directly associated to the number of rules, hence, the "*curse of dimensionality*" problem is significantly reduced. Fig. 3 illustrates the general concept of the proposed CFWNN architecture. Its configuration includes a fuzzy rule base, which consists of a collection of fuzzy IF-THEN rules in the following form:

$$\begin{aligned} R_i: \;& IF\ x_1\ is\ A_{1i}\ and\ x_2\ is\ A_{2i}\ ....and\ x_n\ is\ A_{ni} \\ & THEN\ y_1\ is\ G_1\ and\ ....y_p\ is\ G_p \end{aligned} \tag{1}$$

where $x_1, x_2, ..., x_n$ are input variables, A_{ni} is the i^{th} membership function for the n^{th} input and $G_1, ..., G_p$ are the labels of the fuzzy sets in the output space. Although Gaussian MFs are commonly used in NF systems, their deficiency is their limited ability to localize in the frequency domain. By comparison, the proposed CFWNN, where wavelet functions are utilised, has the ability to localize in both the time and frequency domains. In this paper, the following generalized Mexican Hat wavelet function with translation (μ) and dilation (σ) parameters has been considered as MF:

$$\psi\left(\frac{x-\mu}{\sigma}\right) = \left(1-\left(\frac{x-\mu}{\sigma}\right)^2\right)\exp\left(-0.5\left(\frac{x-\mu}{\sigma}\right)^2\right) \tag{2}$$

Translation parameter determines the center position of the wavelet, while dilation parameter controls the spread of the wavelet. As MF values cannot be negative and larger than unity, the Mexican Hat MF has been normalised / modified as follows:

$$A_{ij} = \frac{\left(1-\left(\frac{x_i-\mu_{ij}}{\sigma_{ij}}\right)^2\right)\exp\left(-0.5\left(\frac{x_i-\mu_{ij}}{\sigma_{ij}}\right)^2\right)+\varepsilon}{1+\varepsilon} \tag{3}$$

where constant $\varepsilon = 0.446$. Fig. 4 illustrates graphically the proposed modified Mexican Hat function.

Figure 4

The structure of the proposed CFWNN is explained below layer by layer:

- **Layer 1:** This layer is simply the input layer. Nodes in this layer pass on the input signals $x_1, x_2, ..., x_n$ to L_2.
- **Layer 2:** This layer is the fuzzification layer, and its nodes represent the fuzzy sets used in the antecedent parts of the fuzzy rules. A fuzzification node receives an input and determines the degree to which this input belongs to in the node's fuzzy set. The outputs of this layer are the values of wavelet MFs for the input values. The modified Mexican Hat MF A_{ij} presented at Eq. 3 has been utilised for the proposed CFWNN, where, index j is

associated with the input variable, while index i is linked with MF's j^{th} input. The initial translation variables μ_{ij} at Eq. 3 are equal to the values of the components of the vectors $\boldsymbol{v_i}$, which come from the second stage of the clustering pre-processing step. The dilation values σ_{ij} are initialised according to

$$\sigma_{ij} = \left(\sum_{k=1}^{n} u_{ik} (x_{kj} - v_{ij})^2 \Big/ \sum_{k=1}^{n} u_{ik} \right)^{1/2} \tag{4}$$

These values are calculated based on the matrix $\mathbf{U}$, where its elements correspond to the fuzzy memberships of $\boldsymbol{x_k}$ in the i^{th} cluster and its values obtained again from the fuzzy c-means part of the clustering step.

- **Layer 3:** This layer is the firing strength calculation layer. Since each fuzzy rule's antecedent part has AND connection operator, the firing strengths are calculated using the product T-norm operator. The most commonly used fuzzy AND operations are intersection and algebraic product (Lee, 1990). In this case, the multiplication has been used, and the output of this layer has the following form:

$$R_j = \prod_{i}^{n} A_{ji}(x_i) \tag{5}$$

The number of nodes, at this layer, is equal to the number of clusters, as it was defined by the clustering pre-processing step.

- **Layer 4**: This layer is the normalization layer. Each node in this layer calculates the normalized activation firing of each rule by:

$$\overline{R}_i = \frac{R_i}{\sum_{j=1}^{c} R_j} \tag{6}$$

The normalized activation firing is the ratio of the activation firing of a given combination to the sum of activation firings of all combinations. It represents the contribution of a given combination to the final result.

- **Layer 5**: This layer is related to the defuzzification/output part of the CFWNN. Each node at this layer combines the output of each node in L_4 by algebraic sum operation after being multiplied by the output weight value w_{ij}:

$$O_i = \sum_{j=1}^{c} w_{ij} \overline{R}_j \tag{7}$$

3.1 Clustering-based Initialisation

The applied clustering algorithm at layer L_2 consists of two stages (Kodogiannis, *et al.,* 2012). In the first stage, the method similar to Learning Vector Quantization (LVQ) algorithm generates crisp c-partitions of the data set. The number of clusters *c* and the cluster centres $v_i,\ i = 1,...,c,$ obtained from this stage are used by Fuzzy *c*-means (FCM) algorithm in the second stage. Fig. 5 illustrates the clustering concept.

The first stage clustering algorithm determines the number of clusters by dividing the learning data into these crisp clusters and calculates the cluster centres which are the initial values of the fuzzy cluster centres derived the second stage algorithm. If we consider that $\boldsymbol{X} = [\boldsymbol{x}_1, ..., \boldsymbol{x}_n] \in \mathrm{R}^{np}$ be a learning data, then the first cluster is created starting with the first data vector from $\boldsymbol{X}$ and the initial value of the cluster centre is taking as a value of this data vector. Then other data vectors are included into the cluster but only these ones which satisfy the following condition

$$\|x_k - v_i\| < D \tag{8}$$

where $x_k \in X, k = 1,...,n$ and $v_i,\ i = 1,...,c$ are cluster centres, $V = [v_1,...,v_n] \in R^{cp}$, the constant value D is fixed at the beginning of the algorithm. Cluster centres v_i are updated for each cluster (i.e., $i = 1,...,c$) according to the following equation

$$v_i(t+1) = v_i(t) + \eta_t(x_k - v_i(t)) \tag{9}$$

where $t = 0,1,2,...$ denotes the number of iterations, $\eta_t \in [0,1]$ is the learning rate and it is decreasing during the execution of the algorithm (depending on the number of elements in the cluster).

Figure 5

At the end of first stage, the number of clusters c is defined, while the dataset is divided into the clusters. In addition, the values of cluster centres $v_i \quad i = 1,...,c$, which can be used as initial values for the second stage clustering algorithm, are calculated. In the second stage the traditional fuzzy *c*-means algorithm has been used to optimize the values of cluster centres.

3.2 CFWNN Learning Phase

The learning algorithm of CFWNN involves the use of the gradient descent (GD) method to optimize the various network parameters. During, the backward "training" passes, the error signals are calculating from the output layer backward to the premise (*i.e.* membership) layers, and parameters at both defuzzification and fuzzification sections are fine-tuned. For each training pair (x, y), the system output O_i is obtained by forward pass after feeding an input pattern into the network. Then the purpose of this learning phase is that, for a given p^{th} training data pair (x_p, y_p), the parameters are adjusted so as to minimise the error function

$$E = \frac{1}{2}\sum_{p=1}^{P}(D_p - O_p)^2 \tag{10}$$

where P is the number of outputs and D_p the desired response of the p^{th} output. Variable O_p is defined as in Eq. 7. According to the GD method, the weights in the defuzzification layer are updated by the following equation

$$\Delta W_{ij} = -\frac{\partial E}{\partial W_{ij}} = -\frac{\partial E}{\partial O_i}\frac{\partial O_i}{\partial W_{ij}} = (D_i - O_i)\bar{R}_j \tag{11}$$

where $i = 1,2,..,p$ and $j = 1,2,..c$ denote the number of output and normalisation units respectively. The weights of the output units are updated according to the following equation

$$W_{ij}(t+1) = W_{ij}(t) + \eta_w \Delta W_{ij} \tag{12}$$

where η_w is the learning rate.

The μ_{ij} and σ_{ij} parameters of the wavelet membership function are adjusted by the amount

$$\begin{aligned} \mu_{ij}(t+1) &= \mu_{ij}(t) - \eta_\mu\left(\frac{\partial E}{\partial \mu_{ij}}\right). \\ \sigma_{ij}(t+1) &= \sigma_{ij}(t) - \eta_\sigma\left(\frac{\partial E}{\partial \sigma_{ij}}\right) \end{aligned} \tag{13}$$

$\frac{\partial E}{\partial \mu_{ij}}$, $\frac{\partial E}{\partial \sigma_{ij}}$ components need to be calculated using the chain rule.

$$\frac{\partial E}{\partial \mu_{ij}} = \frac{\partial E}{\partial \bar{R}_j}\frac{\partial \bar{R}_j}{\partial R_j}\frac{\partial R_j}{\partial A_{ij}}\frac{\partial A_{ij}}{\partial \mu_{ij}},$$
$$\frac{\partial E}{\partial \sigma_{ij}} = \frac{\partial E}{\partial \bar{R}_j}\frac{\partial \bar{R}_j}{\partial R_j}\frac{\partial R_j}{\partial A_{ij}}\frac{\partial A_{ij}}{\partial \sigma_{ij}}, \tag{14}$$

Analytically, the partial derivatives are defined as

$$\frac{\partial E}{\partial \bar{R}_j} = -\sum_{i=1}^{p}\left(D_i - O_i\right)w_{ij} \tag{15}$$

$$\frac{\partial \bar{R}_j}{\partial R_j} = \frac{\sum_{i=1}^{c} R_i - R_j}{\left(\sum_{i=1}^{c} R_i\right)^2} \tag{16}$$

$$\frac{\partial R_j}{\partial A_{ij}} = \prod_{i \neq j} A_{ij} \tag{17}$$

$$\frac{\partial A_{ij}}{\partial \mu_{ij}} = \frac{1}{1+\varepsilon}\left(\frac{\left(x_j - \mu_{ij}\right)}{\left(\sigma_{ij}\right)^2}\left(3 - \frac{\left(x-\mu\right)^2}{\left(\sigma_{ij}\right)^2}\right)\exp\left(-\frac{1}{2}\left(\frac{\left(x-\mu\right)^2}{\left(\sigma_{ij}\right)^2}\right)\right)\right) \tag{18}$$

and

$$\frac{\partial A_{ij}}{\partial \sigma_{ij}} = \frac{1}{1+\varepsilon}\left(\frac{\left(x_j - \mu_{ij}\right)^2}{\left(\sigma_{ij}\right)^3}\left(3 - \frac{\left(x-\mu\right)^2}{\left(\sigma_{ij}\right)^2}\right)\exp\left(-\frac{1}{2}\left(\frac{\left(x-\mu\right)^2}{\left(\sigma_{ij}\right)^2}\right)\right)\right) \tag{19}$$

All modelling schemes have been implemented in MATLAB (ver. R2015a, Mathworks.com).

4. Monitoring Framework Development

A machine learning approach, based on the proposed CFWNN model, has been adopted in order to create a decision support system acting in parallel as an efficient classifier, in an effort to classify meat samples in three quality classes (fresh, semi-fresh, spoiled), as well as a prediction system. The merit of this paper is to propose a learning-based structure which could be considered as a new benchmark method towards the development of efficient intelligent methods in food quality analysis.

Figure 6

For this reason, CFWNN's results are compared with those obtained by MLP neural networks, ANFIS neurofuzzy identification models, support vector machines (SVM) and PLS regression schemes which are considered as well-recognised tools in chemometric analysis. Its overall schematic diagram shown at Fig. 6 includes two CFWNN models for aerobic and MAP storage respectively. Pre-processing of the data acquired from enose sensors is required to create the "olfactory image" of the sample. Generally, this process involves extracting certain significant characteristics from the sensor response curves in order to produce a set of data that can be processed by the recognition system of the enose. Various features can be extracted and utilized in further steps, based on enose's characteristics, such as the type of chemical sensors as well as the stability of their responses to the reference gas, to variations in humidity and temperature levels (Ehret *et al.,* 2011). For this particular experiment, responses as frequency variations $(\Delta \mathrm{f})$, were acquired and in Fig. 7 such responses for all sensor signals classes for meat samples stored at 4°C are shown.

Figure 7

The concept that the discriminating power of an enose depends on the independence amongst its sensors, *i.e.* inversely on their redundancy or cross-correlation, is well documented (Berna *et al.,* 2009). In order to compare the sensor correlations, the pair-wise Pearson correlation between all sensors' responses for the training dataset has been derived. Table 1 illustrates the Pearson correlation matrix among the eight enose sensors. From the eight odorant receptors, only seven were considered as highly correlated (≥ 0.7), with the exclusion of S2. Taking into account that each measurement can be represented as a point in an 8-dimensional space, a dimensionality reduction algorithm has been applied on those enose data used for training purposes.

Table 1

The robust PCA (RPCA) scheme has been utilised to obtain principal components that are not influenced much by outliers. The RPCA is implemented in three main steps. First, the data were pre-processed such that the transformed data are lying in a subspace whose dimension is at most $n-1$. An initial covariance matrix was then constructed and used for selecting the number of components k that will be retained in the sequel, yielding a *k*-dimensional subspace that fits the data well. Then the data points were projected on this subspace where their location and scatter matrix are robustly estimated, from which its k nonzero eigenvalues $l_1,...,l_k$ are computed. The corresponding eigenvectors are the k robust principal components (Hubert *et al.,* 2005). RPCA scheme was implemented in MATLAB, with the aid of PLS_Toolbox (ver. 8.1 Eigenvector.com).

Table 2

For this particular case study, the first four principal components (PC) were associated with the 99% of the total variance, as shown in Table 2. These specific PCs were extracted and utilised as inputs variables to the learning-based models developed for this specific case study, together with information from the various storage temperatures, as well as the related sampling times. Checking however is required to validate the integrity of the developed models in predicting/classifying unknown samples to make sure that models could work in the future for new and similar data. For the aerobic and MAP cases, 140 and 142 samples were considered as training subsets respectively, while the remaining 70 and 71 samples were included in the testing subsets.

As meat quality classification is direct related to microbiological counts and vice versa, a model that combines both these "characteristics" has been considered to be desirable. In order to accommodate both classification and prediction tasks in the same CFWNN structure, the classification task has been modified accordingly. Rather than trying to create a distinct classifier, an attempt has been made to "model" the classes (Kodogiannis, *et al*., 2008). Initially, values of 10, 20 and 30, have been used respectively, to associate the three classes (*i.e*. fresh, semi-fresh and spoiled), with a cluster centre. During the identification process, the output values of $[5.....15]$ were associated to "fresh" class with cluster centre 10, values of $[15.01.....25]$ were associated to "semi-fresh" class with cluster centre 20, and finally values of $[25.01.....35]$ were associated to "spoiled" class with cluster centre 30. The second output node has been assigned to TVC prediction. The classification accuracy of CFWNN models was determined by the number of correctly classified samples in each sensory class divided by the total number of samples in the class. The performance of developed models for TVC prediction for each meat sample was determined by the bias (B_f) and accuracy (A_f) factors, the mean relative percentage residual (MRPE) and the mean absolute percentage residual (MAPR), the root mean squared error (RMSE) and finally the standard error of prediction (SEP) (Panagou, *et al.*, 2007).

5. Results & Discussion

5.1 Aerobic storage case study

CFWNN's structure consists of an input layer which contains six input nodes (i.e. storage temperature, sampling time, and the values of the first four principal components). In the proposed CFWNN model, 10 final rules have been created, using the clustering pre-processing stage. Although GD learning algorithm was utilised as a learning scheme, the training time was completed in less than 1000 epochs, much faster from the equivalent time used to train the MLP neural network. Results revealed that the classification accuracy of the CFWNN model was very satisfactory in the characterization of beef samples, indicating the advantage of a hybrid intelligent approach in tackling complex, nonlinear problems, such as meat spoilage. The classification accuracy is presented in the form of a confusion matrix in Table 3.

Table 3

The model overall achieved a 95.7% correct classification, with 100%, 87.5% and 100% for fresh, semi-fresh and spoiled meat samples, respectively. The sensitivities for fresh and spoiled meat samples reveal zero misclassifications.

Table 4

One spoiled meat sample was accurately classified as spoiled, even marginally and the same situation occurred for one fresh sample. In the case of semi-fresh samples, two samples ("10A7" and "12A7") were misclassified as fresh ones while one semi-fresh sample ("33A5") was misclassified as spoiled one. The "10A7" and "12A7" cases correspond to aerobic samples stored at the same time (12 ^{o}C) and collected at 30h, and 36h respectively. Finally, the "33A5" case corresponds to an aerobic sample stored at 8 ^{o}C and collected at 103h. The specificity index was also high, indicating satisfactory discrimination between these three classes (Table 3). It is characteristic that no fresh samples were misclassified as spoiled and vice versa, indicating that the biochemical information provided by enose data could discriminate at least these two classes accurately. It must be emphasised however that the number of examined samples within each class was not equally distributed, due to the different spoilage rate of beef samples at the different temperatures. The lower accuracies obtained in the semi-fresh class could be explained by the fact that in the evaluation process, sometimes the discrimination between "fresh" and "semi-fresh" class is difficult to be performed accurately.

Figure 8

An MLP network was also constructed for this case study, using the same input vector. The neural network was implemented with two hidden layers (with 12 and 6 nodes respectively) and two output nodes, one for the sensory class and one for the TVC. The model overall achieved a 91.42% correct classification, with 100%, 79.16% and 96.66% for fresh, semi-fresh and spoiled meat samples, respectively. The related sensitivities represent 5 misclassifications out of 24 semi-fresh meat samples, and one misclassification out of 30 spoiled samples, as shown at Table 4. More specifically for the case of semi-fresh samples, four cases were misclassified as fresh cases, while the remaining one as spoiled. Finally, one spoiled sample was misclassified as semi-fresh case.

Table 5

The plot of predicted (via CFWNN) versus observed total viable counts is illustrated in Fig. 8, and shows a very good distribution around the line of equity, with all the testing data included within the ±1 log unit area. Two samples ("8A9", "38A5") have been placed however very close to the borderline. "8A9" sample corresponds to a semi-fresh case stored at 16^{o}C and collected after 24h of storage, while "38A5" corresponds to a spoiled beef sample stored at 8^{o}C and collected after 139h of storage. The performance of the CFWNN model to predict TVCs in beef samples in terms of statistical indices is presented in Table 5. Based on the calculated values of the bias factor B_f, it can be assumed that the

proposed model under-estimated TVCs in fresh and spoiled samples (B_f <1), whereas over-estimation of microbial population for semi-fresh samples was manifested. The mean relative percentage residual index (MRPR) similarly verified the over-prediction for semi-fresh samples (MRPR < 0) and under-prediction for fresh and spoiled samples (MRPR > 0). Finally, the standard error of prediction (SEP) index, a relative typical deviation of the mean prediction values, was 4.57% for the overall samples, indicating a good performance of the network for microbial count predictions. However in the case of fresh samples, the index gave much higher values (i.e. 8.17%).

Figure 9

Although CFWNN model utilises the GD learning method for training, its main advantage over similar systems is related to its MIMO structure capability. Many neuro-fuzzy/fuzzy-wavelet schemes are following the Takagi–Sugeno–Kang (TSK) structure, where only one output is enabled. ANFIS is a well-known representative of TSK-based neuro-fuzzy systems (Jang, *et al.*, 1997). By analysing input/output mapping relationships, ANFIS optimises the distribution of membership functions by using a hybrid learning algorithm. However, ANFIS's main limitation is the exponential growth of rules subjected to the number of input variables. An effective partition of the input space would however decrease the number of rules and thus accelerate training learning speed. A fuzzy rule generation technique that integrates ANFIS with FCM clustering has been applied in this paper in order to minimise the number of fuzzy rules. The FCM is used to systematically create the fuzzy MFs as well as the fuzzy rules for ANFIS. The performance of the proposed model (CANFIS) depends on the optimal number of MFs (clusters). Too few MFs do not allow the CANFIS model to be mapped well, while too many MFs increase the difficulty of training and lead to over-fitting undesirable inputs such as noise.

In addition to CFWNN, a CANFIS as well as an ANFIS model has been developed to predict TVCs. Under the same training conditions, CANFIS performed very satisfactory, while the SEP score of 6.53% for the overall testing samples, is indicating a very good performance of the network for microbial count predictions. It is important to be mentioned, that such performance was achieved with only 7 fuzzy rules. The related plot of the predicted versus the observed TVCs, as shown in Fig. 9, with the majority of data included within the ± 1 log unit area. More specifically, the spoiled "11A11" sample was clearly outside the ± 1 log unit area. "11A11" corresponds to a beef sample stored at 20^{o}C and collected after 32 h of storage. Spoiled sample, "51A1" and semi-fresh sample "26A3" were placed very close to the borderline. "51A1" sample corresponds to a beef sample stored at 0^{o}C and collected after 287 h of storage, while "26A3" corresponds to a beef sample stored at 4^{o}C and collected after 73 h of storage. The performance of the CANFIS model in predicting TVC in meat samples in terms of statistical indices is presented in Table 6. CANFIS model achieved a comparable performance against CFWNN for the semi-fresh case, while divergence was occurred especially for the case of fresh meat samples. An ANFIS scheme was also implemented in order to demonstrate the significance of using a clustering pre-processing stage. Results are shown also at Table 6. ANFIS's performance however was achieved with a high computational cost, by utilizing two membership functions for each input variables and 64 fuzzy rules.

Table 6

In addition to these computational intelligence structures, a multilayer neural network (MLP) and a support vector machine model have been applied to the same case in order reveal the advantage of the proposed advanced learning-based method. The performance of the MLP network in predicting TVC in meat samples in terms of statistical indices is presented in Table 7. The localisation spread through the membership functions, is one advantage of CFWNN and ANFIS-like models against the classic MLP structure.

Support vector machine (SVM) is an alternative machine learning approach based on statistical learning theory (Vapnik, 1998). It has acquired a widely acceptance due to its successful application in classification and regression

tasks (Quan, *et al.*, 2010). The advantages of SVM over MLP models are a global optimal solution and robustness to outliers.

Table 7

The specific SVM used in this paper involves epsilon support vector regression ($\varepsilon - \mathrm{SVR}$). The value of epsilon is used to measure the error between the predicted and real values in a high-dimension space and its value is determined based on practical experience. The objective of SVR is to search for the optimal parameters that minimize the prediction error of the regression model by solving the following optimization problem:

$$\mathrm{L}(\omega, \xi) = \frac{1}{2}\|\omega\|^2 + \mathrm{C}\sum_{i=1}^{n}\xi_i \tag{20}$$

where ω is the weight vector and ξ is a variable that is used to penalize complex fitting functions. The aim of optimisation process is to estimate the parameters ω of the function that give the best-fit of the data. The constant C allows for the penalizing of the error by determining the trade-off between the training error and the model complexity (Al-Anazi, *et al.*, 2010). If C is too large, the algorithm will over-fit the training data; if C is too small then insufficient training will occur.

Appropriate selection of Kernel function at SVR models provides the option of using a non-linear function in inputs space. One specific selection that utilises the radial basis function (RBF) is known as LS-SVMs. The main benefit of LS-SVM is that it is computationally more efficient than the customary SVM method, since the LS-SVM training needs only the solution of a set of linear equations instead of the lengthy and computationally demanding quadratic programming problem that is involved in the standard SVM. The kernel Gaussian function employed at LS-SVM has the following form:

$$\mathrm{K}(\mathrm{x}, \mathrm{x}_i) = \exp\left(-\gamma\|\mathrm{x} - \mathrm{x}_i\|^2\right) \tag{21}$$

where the γ parameter controls the smoothness of the decision boundary in the feature space. For this specific case study, SVR models were implemented in MATLAB using the PLS_Toolbox software and the criterion for the optimal model was defined by the evaluation of SEP index. The C ranges are chosen in between [1 and 1000] and γ value ranges from [0.05 to 1] for training $\varepsilon - \mathrm{SVR}$. The epsilon tolerance value was set to be 0.001. Penalty coefficient C was set at 100, while γ parameter at 0.35. The performance of the SVR model in predicting TVC in meat samples in terms of statistical indices is also presented in Table 7.

Finally, in addition to these learning-based schemes, a partial least squares (PLS) regression scheme has been applied to the same dataset, in order reveal the advantage of advanced learning-based methods. The PLS model was constructed using the same input vector and the PLS_Toolbox software (ver. 8.1, Eigenvector.com) in association with MATLAB was used to perform the PLS analysis. The SIMPLS algorithm has been chosen as the appropriate optimisation scheme. The algorithm calculates the PLS factors directly as linear combinations of the original variables. These factors are determined such as to maximize a covariance criterion, while obeying certain orthogonality and normalization restrictions. The following PLS model is associated with this specific case study.

$$\begin{aligned} \mathrm{Y} \;=\; & 1.81789 + 0.00139 * \mathrm{X}_1 + 0.00098 * \mathrm{X}_2 + 0.00300 * \mathrm{X}_3 \\ & + 0.00387 * \mathrm{X}_4 + 0.23396 * \mathrm{X}_5 + 0.02352 * \mathrm{X}_6 \end{aligned} \tag{22}$$

Although in general, PLS results are worse than those obtained by learning-based schemes, as shown from linear Table 7, such results were expected. It is well known that in modelling of real processes, linear PLS has some difficulties in its practical applications since most real problems are inherently nonlinear and dynamic (Lee, *et al.*, 2006).

5.2 Modified Atmosphere Packaging storage case study

An important advancement in food packaging techniques is the development of Modified Atmosphere Packaging (MAP). Modified atmospheric packaged foods have become increasingly more available, as food manufactures are interested for foods with extended shelf life. In addition to aerobic TVCs prediction, a CFWNN model has been also applied for meat samples packaged under modified atmosphere conditions. For this particular case, 14 final rules have been created, using the clustering pre-processing stage.

Results revealed that although CFWNN's classification accuracy was considered satisfactory in the characterization of beef samples, it was rather inferior compared to the previous aerobic case study. Such accuracy is presented in the form of a confusion matrix in Table 8. The model achieved a 92.95% overall correct classification, and 94.11%, 89.28% and 96.15% for fresh, semi-fresh and spoiled meat samples, respectively. This performance reveals the increased level of difficulty in predicting /classifying meat samples packaged under MAP conditions. Sensitivity information reveals however misclassifications for all categories. One fresh and spoiled meat sample were misclassified as semi-fresh, while three semi-fresh samples were categorised in a different class. Sample "6M11" which corresponds to a fresh sample, stored at 20 ^{o}C and collected at 18h, was classified as semi-fresh, while the spoiled sample "38M5", stored at 8 ^{o}C and collected at 139h, was classified as semi-fresh too. The semi-fresh "36M3" sample, which was stored at 4 ^{o}C and collected at 120h, was classified as fresh class, while semi-fresh "30M7" sample, which was stored at 12 ^{o}C and collected at 91h, was classified as spoiled class. Similarly, the semi-fresh "23M9" case which was stored at 16 ^{o}C and collected at 67h, was classified as spoiled class too.

Table 8

Similarly to the aerobic case, an MLP network was also constructed for this case study, using the same input vector. The neural network was implemented with two hidden layers (with 18 and 10 nodes respectively) and two output nodes, one for the sensory class and one for the TVCs. The model overall achieved a 87.32% correct classification, with 88.23%, 78.57% and 96.15% for fresh, semi-fresh and spoiled meat samples, respectively. Obviously, MLP's classification performance has been deteriorated in this case, revealing the difficulty in modelling meat samples under this specific storage environment.

Table 9

The related sensitivities include 6 misclassifications out of 28 semi-fresh meat samples, one misclassification out of 30 spoiled samples and two misclassifications on fresh samples, as shown at Table 9.

Figure 10

The plot of predicted vs. observed TVCs for MAP spectra is illustrated in Fig 10, and shows a good distribution around the line of equity, with all the data included within the ±1.0 log unit area. Based on Fig. 10, three semi-fresh samples (i.e. "12M11", "54M1", "22M5") were however in the border line of the ±1.0 log unit area. "12M11" corresponds to a beef sample stored at 20^{o}C and collected after 36h of storage, while "54M1" corresponds to a sample stored at 0^{o}C and collected after 359h of storage. Finally, "22M5" case corresponds to a beef sample stored at 8^{o}C and collected after 60h of storage.

Table 10

The performance of the CFWNN model to predict TVCs in beef samples in terms of statistical indices for this case is presented in Table 10. The mean relative percentage residual index (MRPR) revealed an under-prediction for semi-fresh samples (MRPR > 0) and over-prediction for fresh and spoiled samples (MRPR <0). Finally, the standard error of prediction (SEP) index was 5.74% for the overall samples, indicating an inferior performance compared to previous aerobic case.

Table 11

In addition to CFWNN scheme, CANFIS, ANFIS, SVM and MLP models have been developed to predict TVCs for the MAP case. ANFIS model, utilising 64 rules outperformed MLP's prediction performance.

Figure 11

Although ANFIS performed less satisfactory than CFWNN, MLP's performance revealed again its deficiency in handling highly non-linear problems. Prediction from PLS model was similar to the aerobic case study. CANFIS model has shown to have the advantage of requiring fewer rules, in this case requiring only five rules as opposed to the standard ANFIS model. This is a major benefit, since the method is significantly less laborious to construct than the case of ANFIS. The performance of $\varepsilon - \mathrm{SVR}$ model against results provided by MLP and ANFIS-like approaches reveal the robustness of this specific learning-based technique. For the MAP case study, epsilon tolerance and penalty coefficient C were set to 0.001 and 100 respectively, while γ parameter was set at 0.24. The plot of the SVR-based predicted vs. the observed TVCs, as shown in Fig. 11, reveals a good distribution around the line of equity, with the majority of data included within the ± 1 log unit area. Based on Fig. 11, two semi-fresh samples (i.e. "16M5", "13M9") were placed outside the border line of the ±1.0 log unit area. "16M5" corresponds to a beef sample stored at 8^{o}C and collected after 73h of storage, while "13M9" corresponds to a sample stored at 16^{o}C and collected after 42h of storage. Similarly two spoiled samples (i.e. "16M11", "35M9") were placed outside the border line of the ±1.0 log unit area. "16M11" corresponds to a beef sample stored at 20^{o}C and collected after 48h of storage, while "35M9" corresponds to a sample stored at 16^{o}C and collected after 115h of storage. The performance of the SVR model in predicting TVC in meat samples in terms of statistical indices is also presented in Table 11.

6. Conclusion

In conclusion, this simulation study demonstrated the effectiveness of the detection approach based on electronic nose which in combination with an appropriate machine learning strategy could become an effective tool for monitoring meat spoilage during aerobic storage at various temperatures. The collected "volatile" data could be considered as biochemical "signature" containing information for the discrimination of meat samples in quality classes corresponding to different spoilage levels, whereas in the same time could be used to predict satisfactorily the microbial load directly from the sample surface. The realization of this strategy has been fulfilled with the development of a MIMO fuzzy-wavelet network which incorporates a clustering pre-processing stage. Classification performance was very satisfactory, while overall prediction for TVCs has been considered as very promising, although lower performance was observed especially for samples packaged under MAP conditions. Prediction performances of MLP and PLS schemes revealed the deficiencies of these systems which have been used extensively in the area of Food Microbiology, while the SVM's performance revealed its robustness in providing acceptable performances for either aerobic or MAP packaging conditions. There is need to explore further the use of hybrid intelligent systems, and this paper has attempted for the first time to associate enose data with such systems. Research work is in progress to access such intelligent systems utilising only volatile signatures, ignoring thus temperature and time information. Future work will be also focused in incorporating to the data analysis, specific microbiological data, such as *Pseudomonas spp., Brochothrix thermosphacta* and Lactic acid bacteria. Additionally, an ensemble model which will involve many individual learning-based predictors, which will be allocated for the same spoilage detection problem, could enhance the existing prediction accuracy. It has been investigated that ensemble models have advantages with respect single models in terms of better accuracy and robustness for forecasting problems (Li, *et al.*, 2016).

Acknowledgment

The author would like to thank Dr E.Z. Panagou from Agricultural University of Athens, Greece for providing the enose dataset, as well as the related microbiological analysis that correspond to the beef samples.

References

[1] R.H Abiyev, O. Kaynak, Identification and control of dynamic plants using fuzzy wavelet neural networks, Proc. of the IEEE International Symposium on Intelligent Control, (2008), 1295-1301

[2] A. Al-Anazi, I.D. Gates, Support-vector regression for permeability prediction in a heterogeneous reservoirs: SPE 126339, SPE Reserv. Eval. Eng. (2010) 485-495

[3] J.K Amamcharla, S. Panigrahi, C.M. Logue, M. Marchello, J.S. Sherwood, Fourier transform infrared spectroscopy (FTIR) as a tool for discriminating Salmonella typhimurium contaminated beef, Sensing and Instrumentation for Food Quality and Safety, 4 (1) (2010) 1-12

[4] S. Balasubramanian, S. Panigrahi, C.M. Logue, C. Doetkott, M. Marchello, J.S. Sherwood, Independent component analysis-processed electronic nose data for predicting Salmonella typhimurium populations in contaminated beef, Food Control, 19(3) (2008) 236-246

[5] A.Z Berna, A.R Anderson, S.C. Trowell, Bio-benchmarking of electronic nose sensors, PLoS ONE, 4(7) (2009).

[6] D.D.H. Boothe, J.W. Arnold, Electronic nose analysis of volatile compounds from poultry meat samples, fresh and after refrigerated storage, Journal of the Science of Food and Agriculture, 82 (3) (2002) 315-322

[7] L. Capelli, S. Sironi, R. Del Rosso, Electronic noses for environmental monitoring applications, Sensors, 14 (11) (2014) 19979-20007.

[8] A.N. Christiansen, J.M. Carstensen, O. Papadopoulou, N. Chorianopoulos, E.Z. Panagou & G-JE Nychas, Multi spectral imaging analysis for meat spoilage discrimination, 7th International Conference on Predictive Modelling of Food Quality and Safety, Dublin, Ireland, (2011).

[9] C. Di Natale, A. Macagnano, A. D'Amico, Electronic nose and sensorial analysis: Comparison of performances in selected cases, Sensors & Actuators B, 50 (1998) 246–252

[10] C. Di Natale, A. Macagnano, E. Martinelli, R. Paolesse, E. Proietti, A D'Amico, The evaluation of quality of post-harvest oranges and apples by means of an electronic nose, Sensors & Actuators B Chem, 78 (2001) 26–31

[11] B. Ehret, K. Safenreiter, F. Lorenz, J. Biermann, A new feature extraction method for odour classification, Sens. Actuators B Chem. 158 (2011) 75–88

[12] D.I. Ellis, R. Goodacre, Rapid and quantitative detection of the microbial spoilage of muscle foods: current status and future trends, Trends in Food Science & Technology, 12 (2001) 414-424.

[13] R. Fend, A.H.J. Kolk, C. Bessant, P. Buijtels, P.R. Klatser, A.C. Woodman, Prospects for clinical application of electronic-nose technology to early detection of Mycobacterium tuberculosis in culture and sputum, Journal of Clinical Microbiology, 44(6) (2006) 2039-2045

[14] M. Hubert, P. Ousseeuw, K. Branden, ROBPCA: A New Approach to Robust Principal Component Analysis, Technometrics, 47(1) (2005) 64-79

[15] JSR, Jang CT Sun, Mizutani E., Neuro-fuzzy and soft computing: a computational approach to learning and machine intelligence, Prentice-Hall (1997).

[16] L.R. Khot, S. Panigrahi, C. Doetkott, Y. Chang, Evaluation of technique to overcome small dataset problems during neural-network based contamination classification of packaged beef using integrated olfactory sensor system, LWT - Food Science and Technology, 45(2) (2012) 233-240

[17] V.S. Kodogiannis, I. Petrounias, Modelling of survival curves in food microbiology using adaptive fuzzy inference neural networks, 2012 IEEE Int. Conf. on Computational Intelligence for Measurement Systems and Applications (CIMSA 2012), (2012) 35-40

[18] V.S. Kodogiannis, M. Amina, I. Petrounias, A clustering-based fuzzy-wavelet neural network model for short-term load forecasting, Int. Journal of Neural Systems, 23(5) (2013).

[19] V.S. Kodogiannis, A. Alshejari, An Adaptive Neuro-Fuzzy Identification Model for the Detection of Meat Spoilage, Applied Soft Computing, 23 (2014) 483-497

[20] C.C. Lee, Fuzzy logic in control systems: Fuzzy logic controller—Part I & II, IEEE Trans. Syst. Man Cybern.SMC-20, 2 (1990) 404–435.

[21] D.S. Lee, M.W. Lee, S.H. Woo, Y.-J. Kim, J.M. Park, Nonlinear dynamic partial least squares modeling of a full-scale biological wastewater treatment plant, Process Biochemistry, 41(9) (2006) 2050-2057

[22] S. Li, P. Wang, L. Goel, A Novel Wavelet-Based Ensemble Method for Short-Term Load Forecasting with Hybrid Neural Networks and Feature Selection, IEEE Trans. on power systems, 31(3) (2016).

[23] S. Meisel, S. Stöckel, P. Rösch, J. Popp, Identification of meat-associated pathogens via Raman microspectroscopy, Food Microbiology 38 (2014) 36-43

[24] O. Nelles, Nonlinear system Identification: From Classical Approaches to Neura lNetworks and Fuzzy Models, (2001) Springer, Berlin.

[25] M. Nurjuliana, Y.B. Che Man, D. Mat Hashim, A.K.S. Mohamed, Rapid identification of pork for halal authentication using the electronic nose and gas chromatography mass spectrometer with headspace analyzer, Meat Science, 88(4) (2011) 638-644

[26] E.Z. Panagou, V. Kodogiannis, Application of Neural Networks as a Non-linear Modelling Technique in Food Mycology, Expert Systems with Applications 36 (2009) 121-131

[27] O. Papadopoulou, E.Z. Panagou, F. Mohareb, G-J. Nychas, Sensory and microbiological quality assessment of beef fillets, using a portable electronic nose in tandem with support vector machine analysis, Food Research International, 50 (2013) 241–249

[28] T. Quan, X. Liu, Q. Liu, Weighted least squares support vector machine local region method for non linear time series prediction, Appl. Soft Comput. 10(2) (2010) 562–566

[29] P. Skandamis, G.J. Nychas, Preservation of fresh meat with active and modified atmosphere packaging conditions, Int. J Food Microbiology 79 (2002) 35–45.

[30] S. Song, L. Yuan, X. Zhang, K. Hayat, Rapid measuring and modelling flavour quality changes of oxidised chicken fat by electronic nose profiles through the partial least squares regression analysis, Food Chemistry, 141(4) (2013) 4278-4288

[31] F. Tao, Y. Peng, A method for non-destructive prediction of pork meat quality and safety attributes by hyperspectral imaging technique, J Food Eng 126 (2014) 98–106

[32] X. Tian, J. Wang, S. Cui, Analysis of pork adulteration in minced mutton using electronic nose of metal oxide sensors, Journal of Food Engineering, 119(4) (2013) 744-749

[33] V. Vapnik, Statistical Learning Theory, Wiley, New York (1998).

[34] D. Wang, X. Wang, T. Liu, Y. Liu, Prediction of total viable counts on chilled pork using an electronic nose combined with support vector machine, Meat Science, 90 (2012) 373–377

Figures

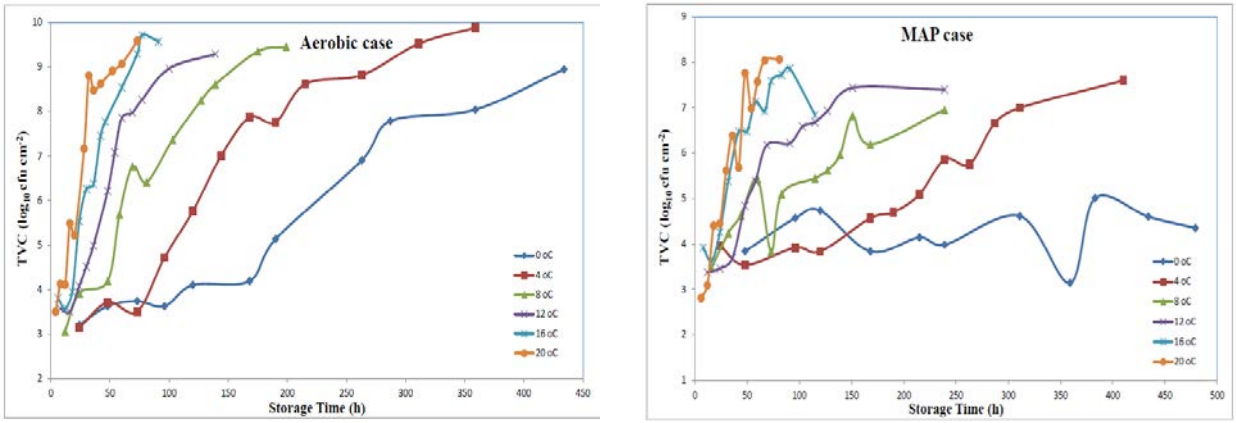

Fig. 1: Population dynamics of TVC at various temperatures for beef samples

Fig. 2: Libra Electronic Nose

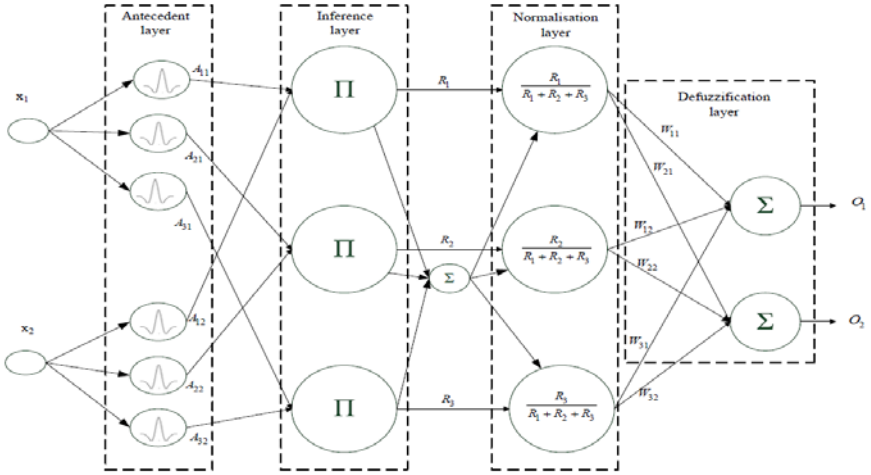

Fig. 3: CFWNN architecture

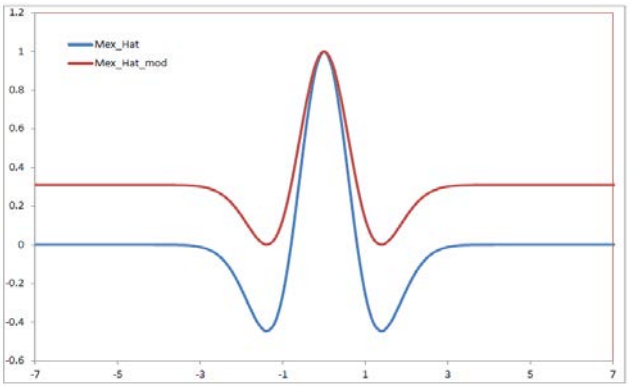

Fig. 4: Mexican Hat wavelet functions

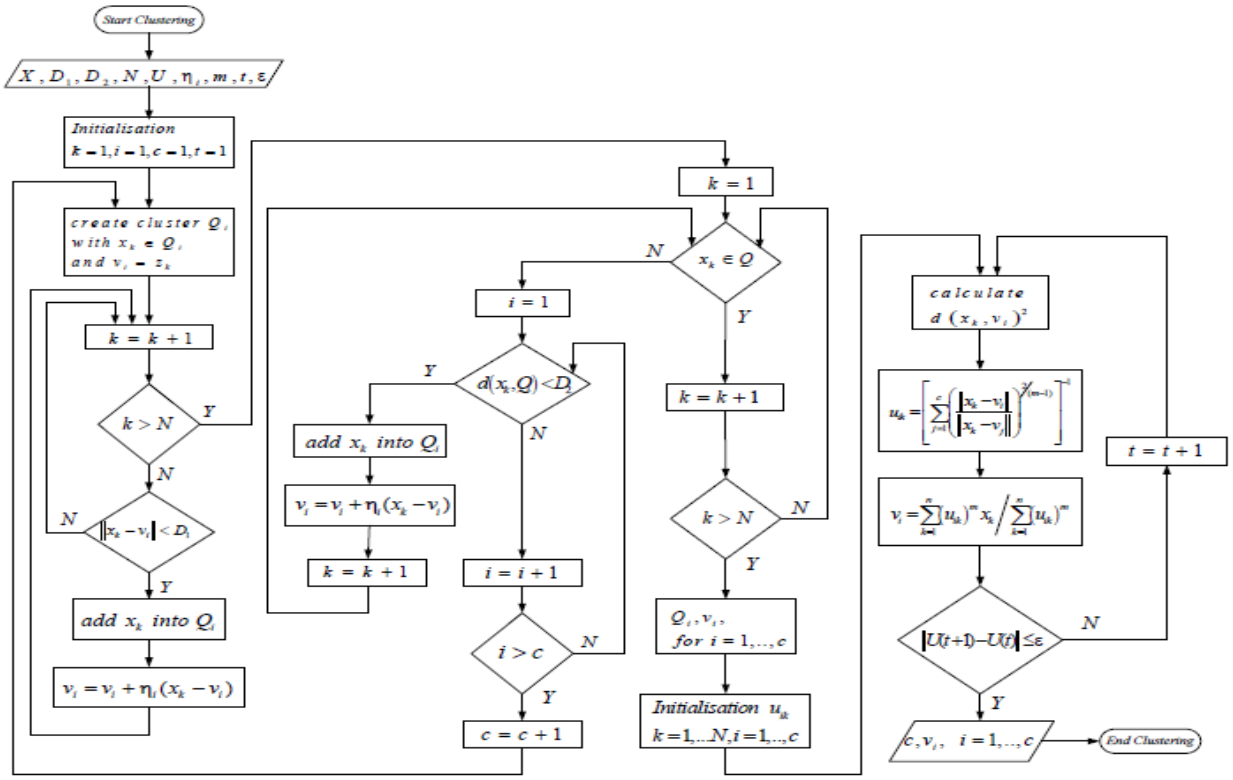

Fig. 5: Clustering concept

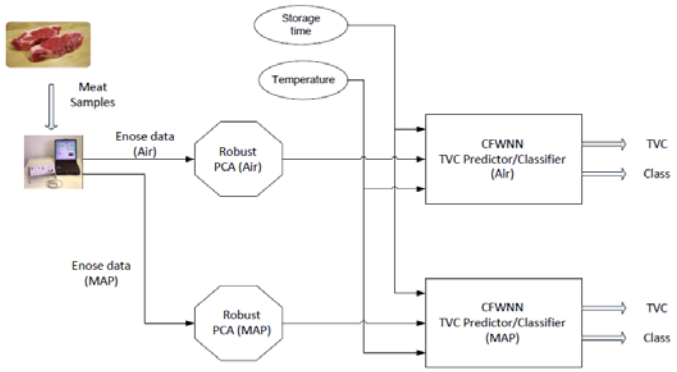

Fig. 6: Structure of proposed decision support system

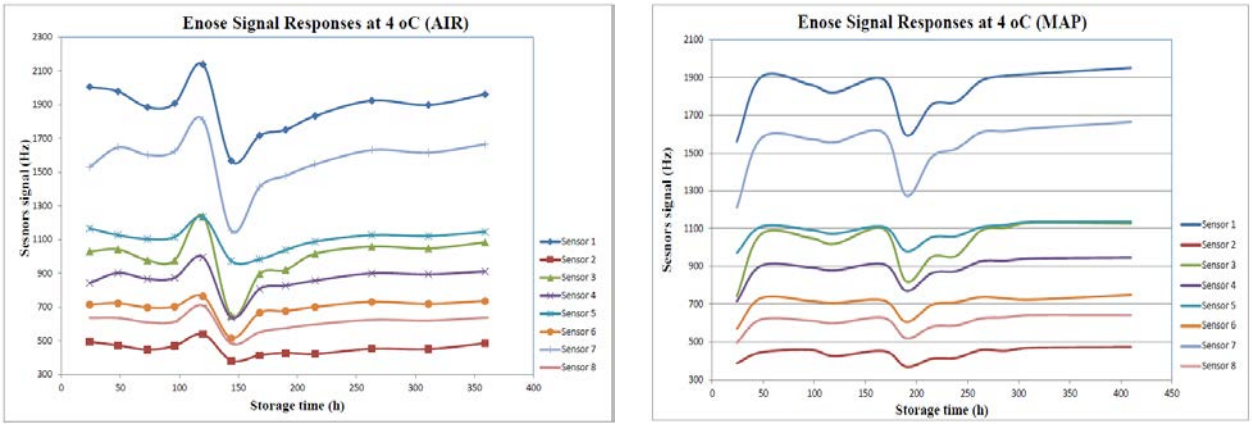

Fig. 7: Enose responses during storage of beef fillets at 4°C

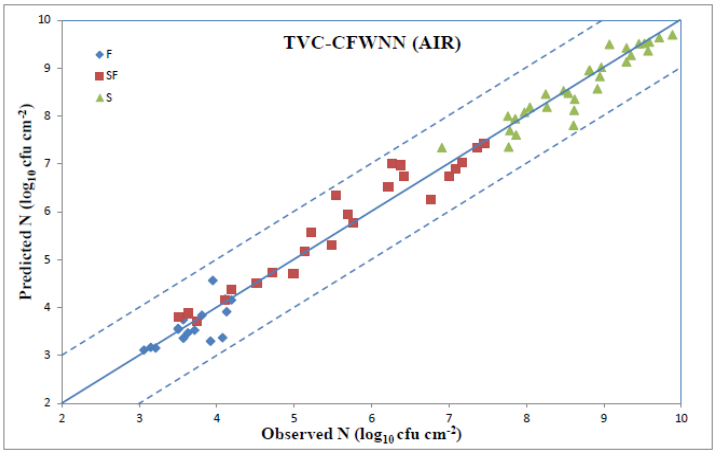

Fig. 8: CFWNN prediction model for TVC (AIR)

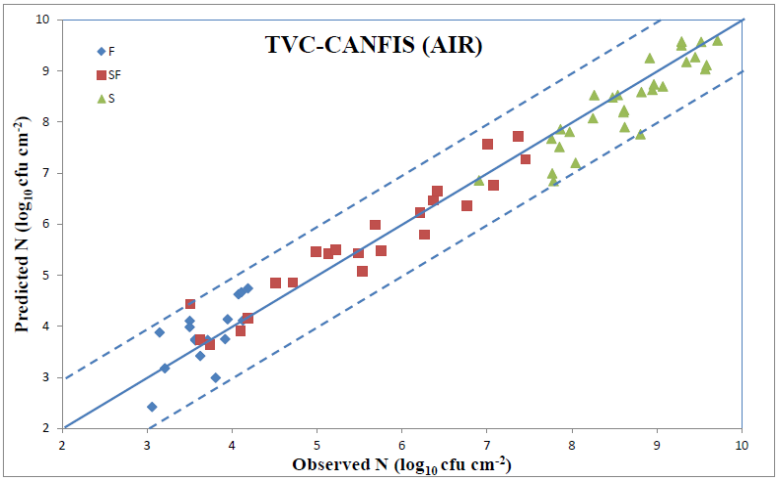

Fig. 9: CANFIS prediction model for TVC (AIR)

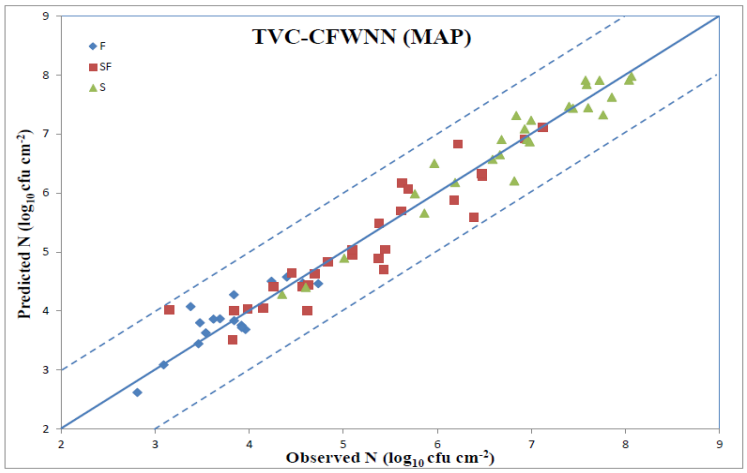

Fig. 10: CFWNN prediction model for TVC (MAP)

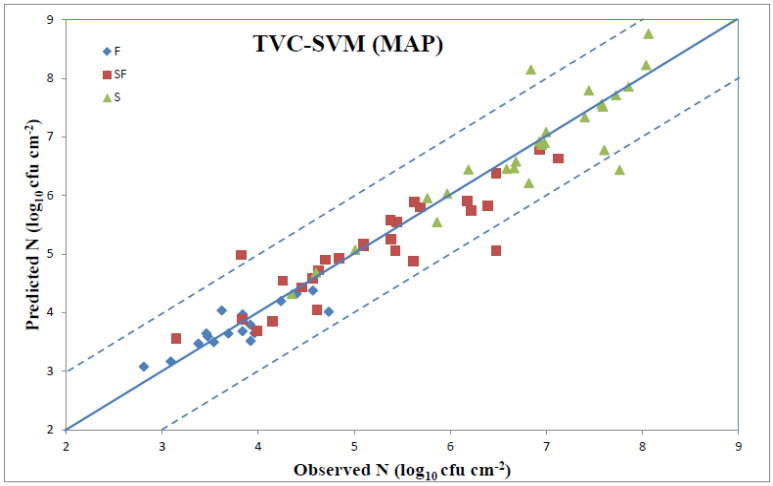

Fig. 11: SVM prediction model for TVC (MAP)

Tables

Sensors (AIR)	S1	S2	S3	S4	S5	S6	S7	S8
S1	1	0.668	0.819	0.704	0.913	0.757	0.961	0.885
S2	0.668	1	0.266	0.134	0.641	0.230	0.586	0.357
S3	0.819	0.266	1	0.937	0.770	0.895	0.867	0.963
S4	0.704	0.134	0.937	1	0.717	0.957	0.811	0.928
S5	0.913	0.641	0.770	0.717	1	0.793	0.907	0.868
S6	0.757	0.230	0.895	0.957	0.793	1	0.849	0.927
S7	0.961	0.586	0.867	0.811	0.907	0.849	1	0.933
S8	0.885	0.357	0.963	0.928	0.868	0.927	0.933	1

Sensors (MAP)	S1	S2	S3	S4	S5	S6	S7	S8
S1	1	0.873	0.635	0.739	0.967	0.835	0.980	0.919
S2	0.873	1	0.313	0.414	0.871	0.542	0.824	0.666
S3	0.635	0.313	1	0.957	0.555	0.875	0.654	0.869
S4	0.739	0.414	0.957	1	0.676	0.949	0.759	0.936
S5	0.967	0.871	0.555	0.676	1	0.781	0.920	0.873
S6	0.835	0.542	0.875	0.949	0.781	1	0.856	0.957
S7	0.980	0.824	0.654	0.759	0.920	0.856	1	0.919
S8	0.919	0.666	0.869	0.936	0.873	0.957	0.919	1

Table 1: Pearson correlation matrix

PCs	Robust PCA		
	Eigenvalue	Prop. %	Cum. prop. %
1	7.17e+004	71.45	71.45
2	1.11e+004	21.88	93.34
3	2.40e+003	4.11	97.45
4	9.47e+002	1.55	99.01

Table 2: Robust PCA scheme

True class (CFWNN)	Predicted class (AIR)			Row total (n_i)	Sensitivity (%)
	Fresh	Semi-fresh	Spoiled		
Fresh ($n = 16$)	15+1(marginal)	0	0	16	100
Semi-fresh ($n = 24$)	2	20+1(marginal)	1	24	87.5
Spoiled ($n = 30$)	0	0	29+1(marginal)	30	100
Column total (n_j)	18	21	31	70	
Specificity (%)	88.88	100	96.77		
Overall correct classification (accuracy): 95.71%					

Table 3: Confusion Matrix for CFWNN acting as classifier (AIR case)

True class (MLP)	Predicted class (AIR)			Row total (n_i)	Sensitivity (%)
	Fresh	Semi-fresh	Spoiled		
Fresh ($n = 16$)	16	0	0	16	100
Semi-fresh ($n = 24$)	4	19	1	24	79.16
Spoiled ($n = 30$)	0	1	29	30	96.66
Column total (n_j)	20	20	30	70	
Specificity (%)	0.80	0.95	96.66		
Overall correct classification (accuracy): 91.42%					

Table 4: Confusion Matrix for MLP acting as classifier (AIR case)

Statistical index (AIR) - CFWNN	Fresh	Semi-fresh	Spoiled	Overall
Mean squared error (MSE)	0.0911	0.1112	0.0681	0.0881
Root mean squared error (RMSE)	0.3019	0.3334	0.2610	0.2969
Mean relative percentage residual (MRPR %)	1.6654	-2.2672	0.5252	-0.1716
Mean absolute percentage residual (MAPR %)	5.2899	4.4713	2.3303	3.7409
Bias factor (B_f)	0.9805	1.0212	0.9943	1.0002
Accuracy factor (A_f)	1.0559	1.0446	1.0238	1.0382
Standard error of prediction (SEP %)	8.1776	5.9582	3.0053	4.5785

Table 5: Performance of CFWNN model for TVC (AIR case)

Statistical index (AIR) - CANFIS	Fresh	Semi-fresh	Spoiled	Overall CANFIS	Overall ANFIS
Mean squared error (MSE)	0.2064	0.1246	0.1958	0.1738	0.2214
Root mean squared error (RMSE)	0.4543	0.3529	0.4425	0.4169	0.4705
Mean relative percentage residual (MRPR %)	-3.5284	-1.5079	2.7259	-0.1552	-1.1780
Mean absolute percentage residual (MAPR %)	10.1934	5.4898	3.9800	5.9178	6.3007
Bias factor (B_f)	1.0276	1.0126	0.9717	0.9982	1.0081
Accuracy factor (A_f)	1.1059	1.0550	1.0419	1.0607	1.0644
Standard error of prediction (SEP %)	12.3061	6.3076	5.0951	6.4292	7.2567

Table 6: Performance of CANFIS/ANFIS models for TVC (AIR case)

Statistical index (AIR)	Overall SVM	Overall MLP	Overall PLS
Mean squared error (MSE)	0.2258	0.2397	1.8587
Root mean squared error (RMSE)	0.4752	0.4896	1.3633
Mean relative percentage residual (MRPR %)	-0.6310	-0.4163	-2.2667
Mean absolute percentage residual (MAPR %)	5.2761	6.2523	20.1221
Bias factor (B_f)	1.0034	1.0002	0.9946
Accuracy factor (A_f)	1.0536	1.0643	1.2126
Standard error of prediction (SEP %)	7.3284	7.5514	21.0263

Table 7: Performance of SVM/MLP/PLS models for TVC (AIR case)

True class (CFWNN)	Predicted class (MAP)			Row total (n_i)	Sensitivity (%)
	Fresh	Semi-fresh	Spoiled		
Fresh ($n = 17$)	15+1(marginal)	1	0	17	94.11
Semi-fresh ($n = 28$)	1	23+2(marginal)	2	28	89.28
Spoiled ($n = 26$)	0	1	24+1(marginal)	26	96.15
Column total (n_j)	17	27	27	71	
Specificity (%)	94.11	92.59	92.59		
Overall correct classification (accuracy): 92.95%					

Table 8: Confusion Matrix for CFWNN acting as classifier (MAP case)

True class (MLP)	Predicted class (MAP)			Row total (n_i)	Sensitivity (%)
	Fresh	Semi-fresh	Spoiled		
Fresh ($n = 17$)	14+1(marginal)	2	0	17	88.23
Semi-fresh ($n = 28$)	2	22	4	28	78.57
Spoiled ($n = 26$)	0	1	25	26	96.15
Column total (n_j)	17	25	29	71	
Specificity (%)	88.23	88	86.2		
Overall correct classification (accuracy): 87.32%					

Table 9: Confusion Matrix for MLP acting as classifier (MAP case)

Statistical index (CFWNN case) MAP	Fresh	Semi-fresh	Spoiled	Overall
Mean squared error (MSE)	0.0737	0.1419	0.0652	0.0975
Root mean squared error (RMSE)	0.2715	0.3767	0.2554	0.3123
Mean relative percentage residual (MRPR %)	-2.0669	0.6115	-0.1570	-0.3112
Mean absolute percentage residual (MAPR %)	5.7326	5.7387	2.9474	4.7151
Bias factor (B_f)	1.0182	0.9907	1.0008	1.0010
Accuracy factor (A_f)	1.0573	1.0589	1.0299	1.0478
Standard error of prediction (SEP %)	7.1594	7.2481	3.7681	5.7401

Table 10: Performance of CFWNN model for TVC (MAP case)

Statistical index (MAP)	Overall CANFIS	Overall ANFIS	Overall SVM	Overall MLP	Overall PLS
Mean squared error (MSE)	0.2063	0.2387	0.1770	0.3029	1.4229
Root mean squared error (RMSE)	0.4542	0.4886	0.4207	0.5503	1.1929
Mean relative percentage residual (MRPR %)	0.0711	0.4371	0.6063	1.2118	-7.2958
Mean absolute percentage residual (MAPR %)	7.1096	6.7719	5.1825	7.8681	20.5115
Bias factor (B_f)	0.9949	0.9912	0.9910	0.9829	1.0411
Accuracy factor (A_f)	1.0731	1.0701	1.0536	1.0831	1.2017
Standard error of prediction (SEP %)	8.3489	8.9815	7.7340	10.1169	21.9282

Table 11: Comparison with alternative models (MAP case)